Published in final edited form as:
Free Radic Biol Med. 2010 April 1; 48(7): 905–914. doi:10.1016/j.freeradbiomed.2010.01.015.

Mitochondrial reserve capacity in endothelial cells: the impact of nitric oxide and reactive oxygen species

Brian P. Dranka[1], **Bradford G. Hill**[1], and **Victor M. Darley-Usmar**[1]

[1]Department of Pathology and Center for Free Radical Biology, University of Alabama at Birmingham, Birmingham, AL 35294

Abstract

The endothelium is not considered to be a major energy requiring organ, but nevertheless endothelial cells have an extensive mitochondrial network. This suggests that mitochondrial function may be important in response to stress and signaling in these cells. In this study, we used extracellular flux analysis to measure mitochondrial function in adherent bovine aortic endothelial cells (BAEC). Under basal conditions, BAEC use only ~35% of their maximal respiratory capacity. We calculate that this represents an intermediate respiratory State between States 3 and 4 which we define as $State_{apparent}$ equal to 3.64. Interestingly, the apparent respiratory control ratio (maximal mitochondrial oxygen consumption/non-ADP linked respiration) in these cells is on the order of 23 which is substantially higher than that which is frequently obtained with isolated mitochondria. These results suggest that mitochondria in endothelial cells are highly coupled and possess a considerable bioenergetic reserve. Since endothelial cells are exposed to both reactive oxygen and nitrogen species (ROS/RNS) in the course of vascular disease, we hypothesized that this reserve capacity is important in responding to oxidative stress. To test this, we exposed BAEC to NO or ROS alone or in combination. We found that exposure to non-toxic concentrations of NO or low levels of hydrogen peroxide generated from 2,3-dimethoxy-1,4-napthoquinone (DMNQ) had little impact on basal mitochondrial function but both treatments reversibly decreased mitochondrial reserve capacity. However, combined NO and DMNQ treatment resulted in an irreversible loss of reserve capacity and was associated with cell death. These data are consistent with a critical role of mitochondrial reserve capacity in endothelial cells in responding to oxidative stress.

Keywords

Atherosclerosis; extracellular flux; reactive nitrogen species; oxidative stress; respiration

Introduction

The endothelium maintains vascular function and is exquisitely sensitive to reactive oxygen and nitrogen species (ROS/RNS) [1,2]. Nitric oxide (NO) is particularly important for cardiovascular health and plays both protective and maladaptive roles in vascular diseases

Corresponding author: Victor Darley-Usmar, Ph.D, Department of Pathology, University of Alabama at Birmingham, Biomedical Research Building II, 901 19th Street South, Birmingham, Alabama 35294, Tel: 205-975-9686, Fax: 205-934-1775, Darley@uab.edu.

associated with oxidative stress. For example, NO has been shown to protect against cell death due to hydrogen peroxide at low concentrations and to enhance the toxicity of ROS at higher concentrations [3–6]. The injurious role of NO in disease has been attributed primarily to biochemical interactions with superoxide ($O_2^{\cdot -}$) to form peroxynitrite ($ONOO^-$), a highly oxidizing species [7]. In the endothelium, NO is derived from endothelial or inducible nitric oxide synthases, and $O_2^{\cdot -}$ is derived from oxidase enzymes or the mitochondrial electron transport chain [8,9]. Interestingly, the concentration and temporal coordination of exposure to these reactive species appear to be particularly important for cell signaling, metabolism, and the commitment of the cell to survival or death [10].

A number of lines of evidence support the hypothesis that mitochondrial respiration can be modulated by the endogenous formation of NO in endothelial cells. Using porcine aortic endothelial cells adhered to microcarrier beads it has been shown that mitochondrial respiration is inhibited by endogenous NO generated from eNOS [11]. Additionally, using permeabilized ECV304 cells, Complex IV-dependent mitochondrial respiration was shown to be inhibited in cells stably transfected with eNOS [12]. An alternative approach has been to induce NO production by transfecting cells with iNOS under the control of a tetracycline inducible promoter [13,14]. Only under conditions of iNOS expression was cellular oxygen consumption inhibited with an apparent IC_{50} for NO of 140nM [14]. A number of *in vivo* studies have also provided evidence that endogenous NO can modulate mitochondrial function [15]. Nevertheless, the detailed molecular mechanisms by which reactive species in combination with NO control mitochondrial function in intact endothelial cells remains incompletely understood.

Mitochondria are of particular interest because they are known to be damaged during the atherosclerotic process [16–18]. This damage appears to be ROS/RNS-dependent and cause loss of bioenergetic control, leading to vascular dysfunction. In most studies, the experimental approach has been to study mitochondria isolated from either heart or liver and assess the impact of ROS/RNS on established mitochondrial bioenergetic parameters such as oxygen consumption and respiratory control. Such studies show that interaction of NO with mitochondria is reversible and occurs primarily at cytochrome *c* oxidase [19,20], is competitive with oxygen [21–23], and is more effective as an inhibitor of oxygen consumption when mitochondria are in State 3 as compared to State 4 respiration [22,24]. While polarographic techniques have been a valuable tool for studies in isolated mitochondria, measuring bioenergetic function in intact cells using this methodology has proved more challenging. The major disadvantage is that the cells must be both continuously stirred and free from matrix attachment. This detached state may result in anoikis which is associated with increased ROS and mitochondrial damage [25]. In addition, non-laminar shear, which occurs as a result of stirring in the oxygen electrode, will result in increased oxidative stress [26,27]. Therefore, an understanding of how mitochondria respond to reactive species in a cellular setting is incomplete.

In this study, we examined the effects of NO and ROS on cellular bioenergetic function in adherent bovine aortic endothelial cells (BAEC). A newly developed, noninvasive technology was used to measure oxygen consumption and extracellular acidification in these cells. This approach made it possible to determine the impact of reactive species on mitochondrial respiration and glycolysis and to characterize the changes in bioenergetics that predispose the cell to injury. We have examined mitochondrial respiratory control in the cells by calculating an apparent respiratory state, analogous to the parameters of State 3 (oxygen consumption sustained by respiratory substrate and ADP) and 4 (respiration sustained solely by respiratory substrates) which are frequently determined with isolated mitochondria. This allows for a more direct comparison to studies with isolated

mitochondria and is particularly useful for endothelial cells where it is not possible to prepare the large quantities of mitochondria needed for polarographic measurements. Using this approach we demonstrate how a basal apparent respiratory control ratio can be determined in the absence or presence of stressors such as ROS/RNS in intact cells. Lastly, the concept of mitochondrial reserve capacity in cells is discussed, with an analysis of the effects of redox stressors on a range of bioenergetic parameters.

Materials and methods

Reagents

DetaNONOate ((*Z*)-1-[2-(2-Aminoethyl)-*N*-(2-ammonioethyl)amino]diazen-1-ium-1,2-diolate) was from Cayman Chemical (Ann Arbor, Ml). DMNQ (2,3-dimethoxy-1,4-napthoquinone) was obtained from Alexis Biochemicals (San Diego, CA). Antimycin A,potassium cyanide, FCCP (carbonyl cyanide 4-(trifluoromethoxy)phenylhydrazone), Oligomycin, Rotenone, and TTFA (thenoyl trifluoroacetone) were all from Sigma (St. Louis, MO) and of the highest grade offered.

Cell culture and treatments

Bovine aortic endothelial cells (BAEC) were harvested from descending thoracic aortas and maintained at 37°C with 5% CO_2 in DMEM growth medium (Mediatech, Manassas, VA) supplemented with 5.5 mM D-Glucose (Sigma, St. Louis, MO) 4 mM glutamine, 1 mM pyruvate, 3.7 g/L sodium bicarbonate 100 U/ml penicillin and 100 ng/ml streptomycin all from Invitrogen (Carlsbad, CA) and 10% fetal bovine serum (FBS, Atlanta Biologicals, Atlanta, GA). Cells used in this study were between passages 5–8. Cells were seeded into Seahorse Bioscience V7 tissue culture plates to the indicated density and allowed to adhere and grow for 24 hours.

Measurements of extracellular flux were made in unbuffered media. For these experiments, the media was changed 1 h prior to the start of the extracellular flux assay to DMEM supplemented with 5.5 mM D-glucose, 4 mM L-glutamine, and 1 mM pyruvate. The pH of the medium was adjusted to 7.4 with NaOH. For MTT assays, BAEC were seeded at 100,000 cells/well in 48-well tissue culture plates. The cells were allowed to adhere and grow for 24 h before being used for experiments. In some experiments, cells were treated with Deta NONOate. Typically, Deta NONOate is prepared in 0.01 N NaOH, so the pH of stocks for treatment in unbuffered media during extracellular flux assays was adjusted to 7.4. The amount of NO released under these conditions was assessed from the spectrophotometric decay of the NONOate (200 μM) measured at 250 nm and found to be 100.00 ± 6.12 pmols/min/well (equivalent to 130nM/min NO). The equivalent rate of production of NO from activated macrophages has been estimated as high as 1 μM per min [28]. Furthermore, production from eNOS is reported to be between 5–200 pmol/min depending upon the stimulus [29].

Measurement of mitochondrial function in BAEC using the XF24-extracellular flux analyzer

A Seahorse Bioscience XF24 Extracellular Flux Analyzer (North Billerica, MA) was used to measure mitochondrial function in intact BAEC. The XF24 creates a transient, 7 μl chamber in specialized microplates that allows for the determination of oxygen and proton concentrations in real time [30,31]. Thus, the rate of oxygen consumption and proton production can be measured across several samples at a time. To allow comparison between different experiments, data are expressed as the rate of oxygen consumption in pmol/min or the rate of extracellular acidification in mpH/min. In some experiments the data were expressed as a percentage of the basal rate of OCR or ECAR. We have found that

mitochondrial function decreases with passage number in BAEC. Therefore, we used cells between passages 5–8 in this study.

Cell Viability

Cell viability was measured by MTT assay as described previously [32], with the following modifications. BAEC were seeded as described above into 48-well culture plates at 100,000 cells/well. After 6 h, the assay media was replaced with media containing 0.4 mg/ml thiazoyl blue tetrazolium (Sigma, St. Louis, MO). The cells were allowed to incubate in a non-CO_2 incubator at 37°C for an additional 2 h. The media was removed, and the resulting formazan crystals were solubilized in 250 µl DMSO. The absorbance was read at 550 nm and the data expressed as a percentage of control cells.

Determination of mitochondrial protein levels

Protein levels of cytochrome *c* oxidase Subunits I and Vb were probed using Western blotting following SDS-PAGE. Briefly, cells were harvested in lysis buffer (10mM Tris, 0.1% Triton X-100, and Complete mini protease inhibitor (Roche Diagnostics, Pleasanton, CA)) and proteins were separated on a 10% SDS-PAGE gel. Levels of cytochrome *c* oxidase Subunits I and Vb were detected using specific antibodies (Invitrogen, Carlsbad, CA).

Results and Discussion

Measurement of Mitochondrial Function in Endothelial Cells

To assess cellular bioenergetics in intact endothelial cells, extracellular flux analysis was used to determine rates of O_2 consumption and glycolysis [30,33]. In the first series of experiments, the optimal number of BAEC needed to obtain a measurable O_2 consumption and extracellular acidification rate (OCR and ECAR) was established (Figure 1A). Both ECAR and OCR showed a proportional response with cell number. For subsequent experiments a seeding density of 40,000 cells per well was selected to allow for optimal detection of changes in OCR and ECAR due to exposure to reactive species. The calculated OCR of approximately 3.02±0.1 nmol/min/10^6 cells (equivalent to 17.4±0.8 nmol/min/mg protein) is reasonably consistent with the published rate of 1.69±0.070 nmol/min/10^6 cells measured by polarography [4]. These rates of mitochondrial oxygen consumption are similar to the values we have obtained using the XF24 for neonatal rat ventricular myocytes (NRVM) of 2.4±0.1 nmol/min/10^6 cells and for rat aortic smooth muscle cells of 3.4±0.1 nmol/min/10^6 cells [34,35]. Interestingly, oxygen consumption in the NRVM equates to 30.6±1.8 nmol/min/mg protein, indicating that the oxygen consumption in these cells is in fact more robust.

Similar to previous reports [36], we defined mitochondrial function in BAEC by sequentially adding pharmacological inhibitors to probe the function of individual components of the respiratory chain. Using 40,000 cells per well, the basal OCR was measured in adherent endothelial cells (Figure 1B). To estimate the proportion of the basal OCR coupled to ATP synthesis, oligomycin (1 µg/ml) was next injected into all samples to inhibit the ATP synthase (Complex V). Typically, the OCR rate decreases in response to oligomycin to the extent to which the cells are using mitochondria to generate ATP. The remaining OCR can be ascribed to both proton leak across the mitochondrial membrane and oxygen consumption by processes other than reduction at cytochrome *c* oxidase. Importantly, oligomycin induces a State 4-like respiratory condition which causes an increase in the mitochondrial membrane potential ($\Delta\psi_m$) [37]. The increased $\Delta\psi_m$ results in higher proton leak through the mitochondrial membrane [38,39], and thus the value determined here for proton leak will be an overestimate as compared to the basal state. Nevertheless, this measurement is useful for comparison between treatment groups and

yields novel information regarding mitochondrial integrity in response to a given treatment. To determine the maximal OCR that the cells can sustain, the proton ionophore (uncoupler) FCCP (1 μM) was injected. As expected, this resulted in stimulation of OCR which occurs as the mitochondrial inner membrane becomes permeable to protons and electron transfer is no longer constrained by the proton gradient across the mitochondrial inner membrane. Lastly, antimycin A (10 μM) is injected to inhibit electron flux through Complex III which causes a dramatic suppression of the OCR. What remains is the OCR that is attributable to O_2 consumption due to the formation of mitochondrial reactive oxygen species and non-mitochondrial sources.

The analysis of the different components of OCR is shown schematically in Figure 1B. This allows calculation of a number of parameters that characterize mitochondrial bioenergetics in intact cells (Figure 1C). The antimycin-independent OCR is subtracted from the values since it represents OCR independent of cytochrome *c* oxidase. The basal rate then represents mitochondrial activity in the cells prior to addition of compounds used to probe bioenergetic function. The addition of oligomycin gives the amount of oxygen consumed that is linked to ATP synthesis. What OCR that remains can be ascribed to either proton leak or the demand on the mitochondrial proton gradient for the movement of ions or metabolites. As noted above, this is likely an over-estimate of proton leak since oligomycin imposes a high mitochondrial membrane potential, enhancing this process. In these cells, non-ATP-linked oxygen consumption constitutes less than 10% of the basal OCR. The OCR after addition of FCCP is an estimate of the potential maximal respiratory capacity. We have noted that high levels of FCCP inhibit mitochondrial respiration presumably due to the loss of the ability to accumulate respiratory substrates. The potential reserve capacity for bioenergetic function in the cells is then the maximal rate minus the basal rate as shown in Figure 1B. It is this parameter which we hypothesize is available to cells for increased work to respond to stress and will be utilized by cells in response to stressors such as ROS/RNS.

These calculations indicate that the cells are normally functioning at a sub-maximal capacity under basal conditions. An important goal of these studies was to relate parameters which are commonly used to describe mitochondrial function in isolated preparations to the actual measurement of mitochondrial function in cells. For example, isolated mitochondria in the presence of ADP and saturating concentrations of substrate are in maximal turnover, and this is termed State 3 respiration. In the absence of ADP, mitochondria in such preparations are in State 2 or 4 respiration, and the consumption of oxygen is due primarily to proton leak. As has been suggested in other studies, it is unlikely that either of these extremes exist for mitochondria in cells; rather some intermediate turnover state, assigned as State 3.5 (the $State_{apparent}$), likely prevails in the cellular context [40]. To determine the apparent respiratory state in endothelial cells, the assumption was made that State 3 respiration was equivalent to the rate measured after addition of FCCP. Similarly, State 4 was assumed to be the rate measured after addition of oligomycin, when the cells are incapable of utilizing the proton gradient to generate ATP due to the presence of the Complex V inhibitor. These assumptions allow for calculation of the apparent respiratory state of these cells under basal conditions. The $State_{apparent}$ can then be calculated from the following equation:

$$State_{apparent} = 4 - \frac{(Basal - Oligo)}{(FCCP - Oligo)}$$

where Basal represents the basal OCR, Oligo represents the Oligomycin-insensitive OCR, and FCCP represents the FCCP-stimulated OCR. This calculation yields an estimate of relative mitochondrial work being used by the cell under the basal condition. As ATP demand is increased, the cells approach State 3 respiration. When ATP/ADP ratios are high

and little mitochondrial respiration is required, the cells are expected to approach State 4. The $State_{apparent}$ allows for an index of where cells fall on this scale following various interventions. Thus, from this calculation an indication of mitochondrial workload can be inferred. Figure 2A displays the $State_{apparent}$ for BAEC as a function of seeding density. Interestingly, the $State_{apparent}$ appears to increase slightly with seeding density. This is likely due to the cells becoming more quiescent with increased density. Thus mitochondrial workload is decreased, and the $State_{apparent}$ approaches 4.

These data can also be used to calculate an apparent respiratory control ratio (RCR) for various metabolic conditions for mitochondria in cells. Using the same assumptions regarding the relative State 3 and 4 respiration in cultured cells, the RCR is calculated as the State 3 rate divided by the State 4 rate. The non-cytochrome *c* oxidase OCR (i.e. in the presence of antimycin; Anti A) was subtracted from all rates.

$$RCR_{basal} = \frac{(Basal - Anti\,A)}{(Oligo - Anti\,A)}$$

$$RCR_{max} = \frac{(FCCP - Anti\,A)}{(Oligo - Anti\,A)}$$

The results of these calculations are shown in Figure 2B. The maximal RCR from these data at a seeding density of 40,000 cells is 23.0 ± 2.7 and under the basal condition is 8.9 ± 0.8.

In addition to the OCR, the ECAR of the medium was also determined as shown in Figure 3A. Importantly, ECAR increased with inhibition of mitochondrial respiration, and this is attributable to the increased requirement for glycolysis for ATP production. Notably, the effect on ECAR was determined to be dose dependent for both oligomycin, and FCCP. Injection of 1 μg/ml oligomycin and 1 μM FCCP was used in this experiment due to the maximal effects those concentrations have on OCR. In independent experiments, the effects of inhibitors of mitochondrial oxidative phosphorylation (10 μM antimycin A, 1 μg/ml oligomycin, 10 μM thenoyl trifluoroacetone (TTFA), 1 mM cyanide, or 1 μM rotenone) on both ECAR and OCR were determined. By plotting OCR vs. ECAR for each of these treatments a profile of the response of these integrated metabolic pathways can be assessed. The control cells under basal conditions are utilizing both glycolysis and oxidative phosphorylation. The addition of mitochondrial inhibitors decreases OCR and stimulates ECAR consistent with the switch from oxidative to glycolytic metabolism (Figure 3B). With the exception of TTFA all of the mitochondrial inhibitors with diverse chemical structures elicit a similar response in the cells. This supports the assumption that these pharmacological inhibitors impact on mitochondrial function as predicted from studies with isolated mitochondria. Interestingly, inhibition of OCR is significantly different after the addition of rotenone (75.0 ± 1.9%) when compared to antimycin A or myxothiazole (approximately 80%), consistent with a major contribution from complex I for cellular respiration under these onditions. The minimal effect of TTFA, a complex II inhibitor, is consistent with a relatively low contribution of succinate to mitochondrial respiration in these cells.

Impact of NO on bioenergetic parameters in endothelial cells

An important physiologically relevant modulator of mitochondrial respiration is NO [41]. We and others have shown in isolated mitochondria that NO-dependent inhibition of respiration at cytochrome *c* oxidase is far greater in State 3 than State 4 [22,24]. These data

suggest that inhibition of mitochondrial respiration in cells will be highly sensitive to the turnover of the respiratory chain. The effect of the apparent intermediate respiratory state occurring in cells, however, has not been examined. Therefore, we determined the impact of NO on the basal OCR using controlled generation of exogenous NO from NO donors. Adherent BAEC were treated with DetaNONOate (0–500 μM) for a period of 1 h prior to measurement of mitochondrial function as described in Figure 1. The levels of NO released by Deta NONOate under these conditions were estimated to be near the higher range for endothelial nitric oxide synthase and well within the levels achieved by the inducible enzyme [42].

As shown in Figure 4A and B, there was no significant effect on the basal OCR with any concentration of DetaNONOate tested, consistent with a lower sensitivity of the respiratory chain to NO when in a low state of turnover. However, on addition of FCCP to stimulate the equivalent of State 3 respiration, OCR was inhibited in an NO-dependent manner (Figure 4C). Since NO-dependent inhibition of cytochrome *c* oxidase is known to increase with decreasing oxygen concentration [43], we determined that the oxygen concentration was the same for all cells before the addition of NO. For example, as shown in Figure 4D inhibition of the FCCP-stimulated rate by NO was evident at the first O_2 measurement after FCCP addition, and persisted over the entire time of measurement. The consequence of the effect of NO on the FCCP stimulated rate was an approximately 4-fold decrease in the reserve respiratory capacity from 94.5 ± 16.5 to 24.6 ± 4.2 pmol O_2/min (Figure 4E). Similarly, the calculated $State_{apparent}$ decreased to 3.32 ± 0.03 in cells treated with 500 μM Deta NONOate, indicating that the cells approached their maximal respiratory capacity after the NO treatment (Figure 5A).

Additionally, the effect of acute NO treatment on ECAR was determined and calculated as the change in mpH/min (Figure 5B). The stimulation of glycolysis was dependent on the concentration of DetaNONOate. This measurement allows for determination of the metabolic profile of BAEC in response to acute exposure to NO as shown in Figure 5C. In contrast to the respiratory chain inhibitors shown in Figure 3 NO modulates the balance between glycolysis and oxidative phosphorylation without evidence of a profound bioenergetic dysfunction at these low levels. Taken together these data extend the findings with isolated mitochondria that the turnover of the respiratory chain is an important determinant in defining the sensitivity to inhibition by NO. A limitation of the present study inherent in the design of the XF24 analyzer is that the experiments were performed at ambient oxygen concentrations which will potentially decrease the ability of NO to inhibit the respiratory chain [21, 22]. This is because NO is both consumed by the mitochondrial inner membrane and competes with oxygen at the active site of cytochrome *c* oxidase [44, 45]. However, since the oxygen levels are several orders of magnitude above the concentrations needed to saturate cytochrome *c* oxidase these higher oxygen concentrations are unlikely to impact on the $State_{apparent}$ of the mitochondria. However, since at lower oxygen levels the autoxidation of NO will be decreased, the available NO to inhibit cytochrome *c* oxidase will increase [46]. This will result in the NO-dependent decrease in reserve capacity being enhanced at lower oxygen tensions.

The effect of ROS formation on mitochondrial reserve capacity in BAEC

Next we examined the effects of acute oxidative stress on mitochondrial bioenergetics by exposing the cells to the redox cycling agent 2,3-dimethoxy-1,4-napthoquinone (DMNQ, 15 μM) for 1 h (Figure 6). DMNQ enters endothelial cells and generates both superoxide and hydrogen peroxide at a rate depending upon its concentration and similar to that generated by enzymes such as NADPH oxidase [47]. We have previously shown that this concentration will induce cell death through an apoptotic process in BAEC if exposure proceeds longer that 3–4 h [4]. As shown in Figure 6A and B, DMNQ stimulated the basal

OCR, and this stimulation was partially independent of the addition of mitochondrial inhibitors. This indicates that the increase in oxygen consumption is largely due to the redox cycling of DMNQ and not a stimulation of the mitochondrial electron transport chain. Additionally, under these conditions, DMNQ alone has a stimulatory effect on proton leak-dependent OCR (Figure 6C). Importantly, DMNQ inhibited the FCCP-induced oxygen consumption in a concentration-dependent manner. This combined with the increased basal OCR to result in a significant decrease in the reserve capacity (Figure 6D). This furthermore led to a decrease in the $State_{apparent}$ as the cells lost their maximal respiratory capacity (Figure 6E).

As a control for the requirement of redox cycling for DMNQ-stimulated oxygen consumption, the flavoprotein inhibitor diphenyleneiodonium (DPI, 10 μM) was added and found to prevent the DMNQ-dependent increase in basal OCR (Fig. 6F). Interestingly, DPI itself slightly inhibited the induction of the OCR due to FCCP treatment, consistent with an increased electron flux through complex I. No significant change in the basal ECAR was detected under any of the treatment conditions with DMNQ (data not shown).

The combined effect of NO and DMNQ on mitochondrial function in BAEC

In the previous experiments we have demonstrated that both DMNQ and NO are capable of decreasing the mitochondrial reserve capacity; however, these species by themselves do not impact significantly on the basal OCR. Under conditions of inflammation, endothelial cells are exposed to both NO and ROS, and this was modeled in the next series of experiments. As shown in Figure 7A, the cells were exposed to a combination of 250 μM Deta NO and 15 μM DMNQ for 60 min, and mitochondrial function analyzed. This resulted in an increase in proton leak on addition of oligomycin and a failure to stimulate oxygen consumption on the addition of FCCP (Figure 7B). In this case we cannot rule out an exacerbation of the underlying bioenergetic defect due to addition of oligomycin. Importantly, these effects on mitochondrial function do not appear to be due to cellular production of ROS, as there is no increase in the antimycin A-insensitive OCR (Figure 7C). To determine the long term effects of this treatment regimen on cells, we next examined cell viability. As shown in Figure 7D, BAEC were treated with the indicated concentrations of DMNQ and/or Deta NONOate for 6 h. DMNQ decreased cell survival at concentrations above 7.5 μM whereas the Deta NONOate (500 μM) had a small but significant effect in the absence of DMNQ. In the presence of both the $NO^{\cdot}$ donor and DMNQ however, toxicity was greatly increased, and significant decreases in cell survival were observed with as little as 5 μM DMNQ when in combination with the $NO^{\cdot}$ donor.

Can inhibition of reserve capacity be reversed following removal of Deta NONOate or DMNQ?

Next we tested whether the effects on reserve capacity mediated by ROS/RNS are reversible. Mitochondrial function was analyzed following removal and wash out of the Deta NONOate and DMNQ. As shown in Figure 8A, with NO as an example, the ROS/RNS generators were added for a period of one hour followed by a 30-minute washout before measurement of OCR and the addition of oligomycin, FCCP, and antimycin A as described previously. We found that the wash procedure had a small but consistent effect in decreasing maximal OCR in controls. For this reason the data is expressed as the percentage of the appropriate control. As shown in Figure 8B,C, the inhibitory effects on OCR in response to Deta NONOate (250 μM) and DMNQ (15 μM) are reversed following the washout period. Interestingly, the effect of the combined treatment with 250 μM Deta NONOate and 15 μM DMNQ was not reversible (Figure 8D).

We have previously shown that chronic exposure to NO can decrease mitochondrial proteins in endothelial cells but the impact on mitochondrial function was not determined [48]. In the next series of experiments, the effects of a longer-term treatment with Deta NONOate were then examined to determine if there is any point beyond which the effects of NO are irreversible. BAEC seeded into XF plates as described were treated with 0–500 μM Deta NONOate for 4 or 16 h. The cells were washed free of the NO donor, and basal oxygen consumption was then measured. As shown in Figure 9A,B basal OCR was not significantly inhibited at 4 h, but was markedly decreased after 16 h, even at the lowest concentration of Deta NONOate tested. To determine if the inhibition of basal OCR was a result of decreased mitochondrial protein, BAEC seeded into 6-well plates were treated with 0–500 μM Deta NONOate for 16 h. The cells were then harvested, and protein levels of cytochrome *c* oxidase Subunits I and Vb were probed by Western blot. As shown in Figure 9C, total levels of both of these proteins were decreased by up to 60%.

Summary

In this study, we have demonstrated the development of an assay for determination of mitochondrial function in intact endothelial cells. These experiments show that BAEC have basal O_2 consumption rates that are only ~35% of the maximal oxygen consumption achievable using the uncoupler FCCP. This indicates the presence of a reserve or spare respiratory capacity that is available for the cells to call upon when bioenergetic demand is increased. BAEC in culture normally consume oxygen in an intermediate State between State 3 and 4 [49,50], which we calculate to be approximately $State_{apparent}$ 3.6. It is of note that the calculated RCR values for these cells indicate that the mitochondria are tightly coupled, under normal physiological conditions. Importantly, this indicates that the endothelium *in vivo* may be well poised to offer protection against oxidative and nitrosative stress that typically occurs in the vasculature during the pathological processes associated with vascular dysfunction.

It is well established that NO is a reversible inhibitor of the mitochondrial respiratory chain, and it has been demonstrated by a number of laboratories that cellular oxygen consumption can be decreased in response to the endogenous generation of NO from intracellular NO synthases [42]. However, the impact of NO on other mitochondrial parameters such as proton leak and the respiratory reserve capacity is not known. In this study, we measured respiratory function in adherent endothelial cells in the presence and absence of exogenously produced nitric oxide. The development of an assay to quantify mitochondrial function allowed for direct analysis of the effects of nitric oxide beyond the inhibition of cytochrome *c* oxidase. In addition, estimation of the functional consequence of cytochrome *c* oxidase inhibition reveals profound effects on overall cellular bioenergetics. Specifically, a loss of mitochondrial reserve capacity is expected to lead to decreased ability to respond to secondary energetic stressors. Exposure to nitric oxide at high concentrations *in vivo* then could lead to an impaired ability to cope with oxidant stress. This scenario may occur in diseases such as atherosclerosis where the endothelium is exposed to high concentrations of NO and oxidants such as superoxide and hydrogen peroxide. Importantly, we have for the first time modeled this scenario to determine the effects of co-exposure to NO and ROS on cellular bioenergetics. These data demonstrate the large increase in proton leak that occurs upon co-treatment that decreases the efficiency of mitochondrial ATP generation. These experiments demonstrated that transient exposure to nitric oxide or ROS generated by DMNQ results in reversible inhibition of the reserve capacity; however, co-treatment resulted in irreversible inhibition of OCR. The reversible inhibition by NO is consistent with the interaction with cytochrome *c* oxidase, and reversibility in response to ROS would be consistent with reversible protein modification such as *S*-thiolation. In support of this argument, we have recently shown that enhancing *S*-glutathiolation in cells decreased

reserve capacity [35]. The acute irreversible effects of the combined NO and DMNQ treatment could be ascribed to a number of mechanisms including *S*-nitrosation of complex I or tyrosine nitration or protein oxidation of other respiratory complexes [51].

The data presented here have broad application to the understanding of cellular bioenergetic function *in vitro* and importantly add to our knowledge of the whole-cell response to oxidative stress. We hypothesize that the damage to mitochondrial DNA associated chronic inflammatory conditions that affect the vasculature will also contribute to decreased bioenergetic reserve capacity rendering the cells more sensitive to oxidative stress. It follows that novel therapeutic strategies could be developed which enhance mitochondrial reserve capacity in the vasculature for the treatment of hypertension and atherosclerosis.

Abbreviations

Deta NONOate	Deta NO (*Z*)-1-[2-(2-Aminoethyl)-*N*-(2-ammonioethyl)amino]diazen-1-ium-1,2-diolate
DMNQ	2,3-dimethoxy-1,4-naphthoquinone
DPI	diphenyleneiodonium
FCCP	Carbonyl cyanide 4-(trifluoromethoxy)phenylhydrazone
MTT	Thiazolyl Blue Tetrazolium Bromide
$NO^{\cdot}$	nitric oxide
$ONOO^{-}$	peroxynitrite
RCR	Respiratory Control Ratio
ROS/RNS	Reactive Oxygen Species/Reactive Nitrogen Species
SDS-PAGE	Sodium Dodecyl Sulfate-Polyacrylamide Gel Electrophoresis
TTFA	thenoyl trifluoroacetone

References

1. Palmer RMJ, Ferrige AG, Moncada S. Nitric oxide release accounts for the biological activity of endothelium-derived relaxing factor. Nature 1987;327(6122):524–526. [PubMed: 3495737]
2. Lee MY, Griendling KK. Redox signaling, vascular function, and hypertension. Antioxid Redox Signal 2008;10(6):1045–1059. [PubMed: 18321201]
3. Ramachandran A, et al. Inhibition of mitochondrial protein synthesis results in increased endothelial cell susceptibility to nitric oxide-induced apoptosis. PNAS 2002;99(10):6643–6648. [PubMed: 12011428]
4. Ramachandran A, et al. Activation of c-Jun N-Terminal Kinase and Apoptosis in Endothelial Cells Mediated by Endogenous Generation of Hydrogen Peroxide. Biological Chemistry 2002;383(3): 693. [PubMed: 12033458]
5. Kotamraju S, et al. Nitric oxide inhibits H2O2-induced transferrin receptor-dependent apoptosis in endothelial cells: Role of ubiquitin-proteasome pathway. PNAS 2003;100(19):10653–10658. [PubMed: 12958216]
6. Kotamraju S, et al. Nitric oxide mitigates peroxide-induced iron-signaling, oxidative damage, and apoptosis in endothelial cells: role of proteasomal function? Arch Biochem Biophys 2004;423(1): 74–80. [PubMed: 14989268]
7. Beckman JS, et al. Apparent hydroxyl radical production by peroxynitrite: implications for endothelial injury from nitric oxide and superoxide. Proc Natl Acad Sci U S A 1990;87(4):1620–1624. [PubMed: 2154753]

8. Paravicini TM, Touyz RM. NADPH oxidases, reactive oxygen species, and hypertension: clinical implications and therapeutic possibilities. Diabetes Care 2008;31:S170–S180. [PubMed: 18227481]
9. Lambert AJ, Brand MD. Reactive oxygen species production by mitochondria. Methods Mol Biol 2009;554:165–181. [PubMed: 19513674]
10. Wiseman DA, et al. Alterations in zinc homeostasis underlie endothelial cell death induced by oxidative stress from acute exposure to hydrogen peroxide. Am J Physiol Lung Cell Mol Physiol 2007;292(1):L165–L177. [PubMed: 16936243]
11. Clementi E, et al. On the mechanism by which vascular endothelial cells regulate their oxygen consumption. PNAS 1999;96(4):1559–1562. [PubMed: 9990063]
12. Paxinou E, et al. Dynamic regulation of metabolism and respiration by endogenously produced nitric oxide protects against oxidative stress. Proc Natl Acad Sci USA 2001;98(20):11575–11580. [PubMed: 11562476]
13. Mateo J, et al. Regulation of hypoxia-inducible factor-1alpha by nitric oxide through mitochondria-dependent and -independent pathways. Biochem J 2003;376(Pt 2):537–544. [PubMed: 14531732]
14. Rodriguez-Juarez F, Aguirre E, Cadenas S. Relative sensitivity of soluble guanylate cyclase and mitochondrial respiration to endogenous nitric oxide at physiological oxygen concentration. Biochem J 2007;405(2):223–231. [PubMed: 17441787]
15. Loke KE, et al. Nitric oxide modulates mitochondrial respiration in failing human heart. Circulation 1999;100(12):1291–1297. [PubMed: 10491373]
16. Ramachandran A, et al. Mitochondria, nitric oxide, and cardiovascular dysfunction. Free Radic Biol Med 2002;33(11):1465–1474. [PubMed: 12446203]
17. Ballinger SW. Mitochondrial dysfunction in cardiovascular disease. Free Radic Biol Med 2005;38(10):1278–1295. [PubMed: 15855047]
18. Madamanchi NR, Runge MS. Mitochondrial Dysfunction in Atherosclerosis. Circ Res 2007;100(4):460–473. [PubMed: 17332437]
19. Torres J, Darley-Usmar V, Wilson MT. Inhibition of cytochrome c oxidase in turnover by nitric oxide: mechanism and implications for control of respiration. Biochem J 1995;312(Pt 1):169–173. [PubMed: 7492308]
20. Cooper CE, et al. Nanotransducers in cellular redox signaling: modification of thiols by reactive oxygen and nitrogen species. Trends Biochem Sci 2002;27(10):489–492. [PubMed: 12368076]
21. Brown GC, Cooper CE. Nanomolar concentrations of nitric oxide reversibly inhibit synaptosomal respiration by competing with oxygen at cytochrome oxidase. FEBS Letters 1994;356(2–3):295–298. [PubMed: 7805858]
22. Brookes PS, et al. Control of mitochondrial respiration by NO*, effects of low oxygen and respiratory state. J Biol Chem 2003;278(34):31603–31609. [PubMed: 12788936]
23. Antunes F, Boveris A, Cadenas E. On the mechanism and biology of cytochrome oxidase inhibition by nitric oxide. Proceedings of the National Academy of Sciences of the United States of America 2004;101(48):16774–16779. [PubMed: 15546991]
24. Borutaite V, Brown GC. Rapid reduction of nitric oxide by mitochondria, and reversible inhibition of mitochondrial respiration by nitric oxide. Biochem J 1996;315(Pt 1):295–299. [PubMed: 8670121]
25. Li AE, et al. A Role for Reactive Oxygen Species in Endothelial Cell Anoikis. Circ Res 1999;85(4):304–310. [PubMed: 10455058]
26. De Keulenaer GW, et al. Oscillatory and steady laminar shear stress differentially affect human endothelial redox state: role of a superoxide-producing NADH oxidase. Circ Res 1998;82(10): 1094–1101. [PubMed: 9622162]
27. Hwang J, et al. Oscillatory shear stress stimulates endothelial production of O2- from p47phox-dependent NAD(P)H oxidases, leading to monocyte adhesion. J Biol Chem 2003;278(47):47291–47298. [PubMed: 12958309]
28. Laurent M, Lepoivre M, Tenu JP. Kinetic modelling of the nitric oxide gradient generated in vitro by adherent cells expressing inducible nitric oxide synthase. Biochem J 1996;314(Pt 1):109–113. [PubMed: 8660270]
29. Malinski T. Understanding nitric oxide physiology in the heart: a nanomedical approach. Am J Cardiol 2005;96(7B):13i–24i. [PubMed: 15979424]

30. Ferrick DA, Neilson A, Beeson C. Advances in measuring cellular bioenergetics using extracellular flux. Drug Discov Today 2008;13(5–6):268–274. [PubMed: 18342804]
31. Gerencser AA, et al. Quantitative Microplate-Based Respirometry with Correction for Oxygen Diffusion. Anal Chem. 2009
32. Mosmann T. Rapid colorimetric assay for cellular growth and survival: application to proliferation and cytotoxicity assays. J Immunol Methods 1983;65(1–2):55–63. [PubMed: 6606682]
33. Wu M, et al. Multiparameter metabolic analysis reveals a close link between attenuated mitochondrial bioenergetic function and enhanced glycolysis dependency in human tumor cells. Am J Physiol Cell Physiol 2007;292(1):C125–C136. [PubMed: 16971499]
34. Hill BG, et al. Importance of the bioenergetic reserve capacity in response to cardiomyocyte stress induced by 4-hydroxynonenal. Biochem J 2009;424(1):99–107. [PubMed: 19740075]
35. Hill BG, et al. Regulation of vascular smooth muscle cell bioenergetic function by protein glutathiolation. Biochim Biophys Acta. 2009 doi:10.1016/j.bbabio.2009.11.005.
36. Jekabsons MB, Nicholls DG. In situ respiration and bioenergetic status of mitochondria in primary cerebellar granule neuronal cultures exposed continuously to glutamate. J Biol Chem 2004;279(31):32989–33000. [PubMed: 15166243]
37. Brown GC, Lakin-Thomas PL, Brand MD. Control of respiration and oxidative phosphorylation in isolated rat liver cells. Eur J Biochem 1990;192(2):355–362. [PubMed: 2209591]
38. Brand MD. The proton leak across the mitochondrial inner membrane. Biochim Biophys Acta 1990;1018(2–3):128–133. [PubMed: 2393654]
39. Brown GC. The leaks and slips of bioenergetic membranes. Faseb J 1992;6(11):2961–2965. [PubMed: 1644259]
40. Choi SW, Gerencser AA, Nicholls DG. Bioenergetic analysis of isolated cerebrocortical nerve terminals on a microgram scale: spare respiratory capacity and stochastic mitochondrial failure. J Neurochem 2009;109(4):1179–1191. [PubMed: 19519782]
41. Cooper CE. Competitive, reversible, physiological? Inhibition of mitochondrial cytochrome oxidase by nitric oxide. IUBMB Life 2003;55(10–11):591–597. [PubMed: 14711004]
42. Balbatun A, Louka FR, Malinski T. Dynamics of nitric oxide release in the cardiovascular system. Acta Biochim Pol 2003;50(1):61–68. [PubMed: 12673347]
43. Borutaite V, et al. Reversible inhibition of cellular respiration by nitric oxide in vascular inflammation. Am J Physiol Heart Circ Physiol 2001;281(6):H2256–H2260. [PubMed: 11709390]
44. Shiva S, et al. Nitric oxide partitioning into mitochondrial membranes and the control of respiration at cytochrome c oxidase. PNAS 2001;98(13):7212–7217. [PubMed: 11416204]
45. Cooper CE, Giulivi C. Nitric oxide regulation of mitochondrial oxygen consumption II: Molecular mechanism and tissue physiology. Am J Physiol Cell Physiol 2007;292(6):C1993–C2003. [PubMed: 17329402]
46. Joshi MS, et al. Nitric oxide is consumed, rather than conserved, by reaction with oxyhemoglobin under physiological conditions. Proc Natl Acad Sci U S A 2002;99(16):10341–10346. [PubMed: 12124398]
47. Watanabe N, Forman HJ. Autoxidation of extracellular hydroquinones is a causative event for the cytotoxicity of menadione and DMNQ in A549-S cells. Archives of Biochemistry and Biophysics 2003;411(1):145–157. [PubMed: 12590933]
48. Ramachandran A, Ceaser E, Darley-Usmar VM. Chronic exposure to nitric oxide alters the free iron pool in endothelial cells: Role of mitochondrial respiratory complexes and heat shock proteins. PNAS 2004;101(1):384–389. [PubMed: 14691259]
49. Korzeniewski B, Mazat JP. Theoretical studies on the control of oxidative phosphorylation in muscle mitochondria: application to mitochondrial deficiencies. Biochem J 1996;319(Pt 1):143–148. [PubMed: 8870661]
50. Korzeniewski B. Simulation of state 4 --> state 3 transition in isolated mitochondria. Biophys Chem 1996;57(2–3):143–153. [PubMed: 17023337]
51. Burwell LS, et al. Direct evidence for S-nitrosation of mitochondrial complex I. Biochem J 2006;394(Pt 3):627–664. [PubMed: 16371007]

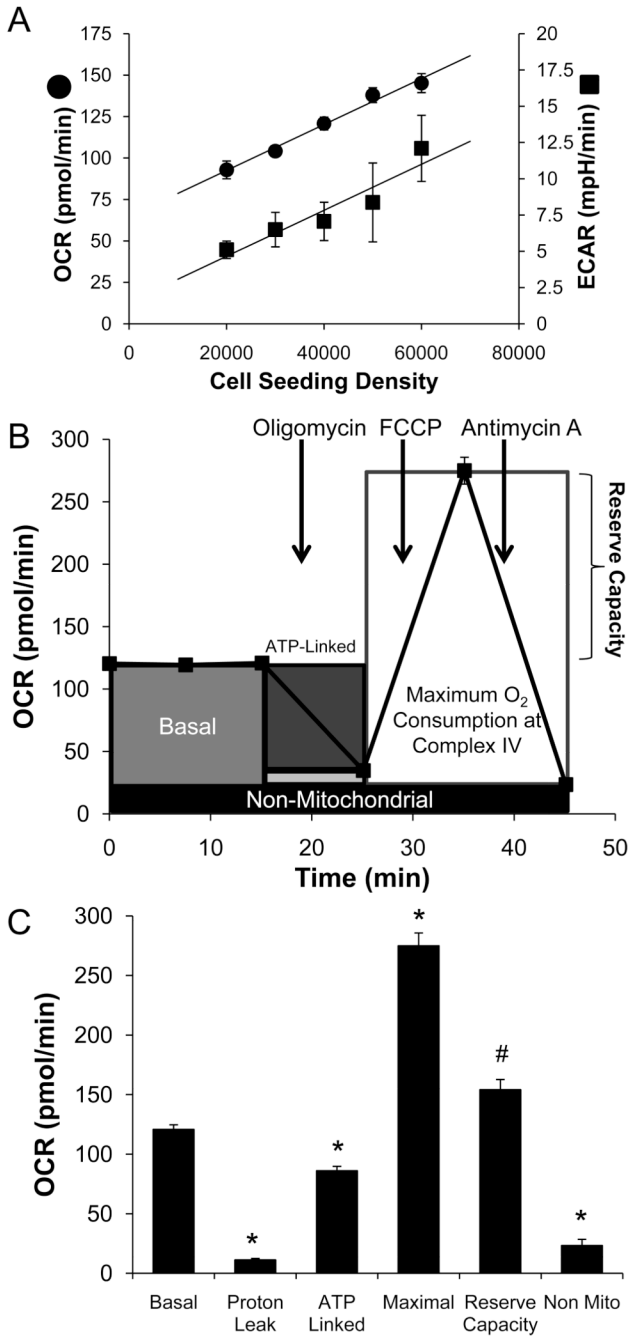

Figure 1. Measurement of Mitochondrial Function in BAEC using the XF24 analyzer

Seahorse Bioscience V7 Tissue Culture Plates were seeded with BAEC (20,000–60,000 cells/well) and allowed to grow for 24 h before the measurement of OCR and ECAR. Panel A: Basal OCR and ECAR were measured three times and plotted as a function of cell seeding number. Panel B represents the time course for measurement of OCR for 40,000 cells under the basal condition followed by the sequential addition of oligomycin (1 μg/ml), FCCP (1 μM), and antimycin A (10 μM) with a measurement of OCR and ECAR as indicated. This progress curve is annotated to show the relative contribution of non-respiratory chain oxygen consumption, ATP-linked oxygen consumption, the maximal OCR after the addition of FCCP, and the reserve capacity of the cells. The contribution of each of

these parameters to the total cellular oxygen consumption is plotted in Panel C. All data are the mean ± sem, n≥3 per group. *, p<0.05 vs. Control; #, p<0.05 vs. Maximal OCR.

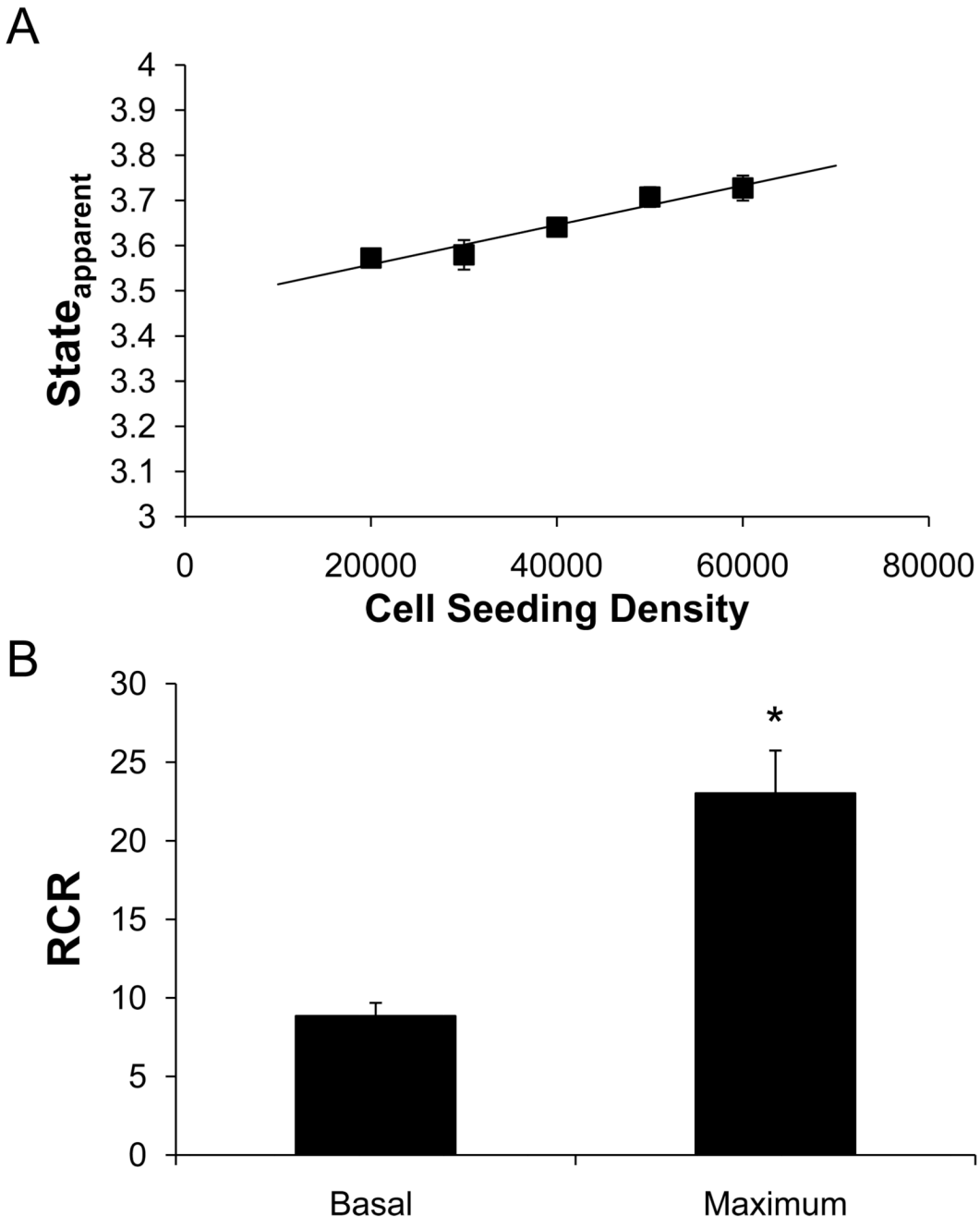

Figure 2. Apparent respiratory state increases with cell density

Panel A: The $State_{apparent}$ was calculated for cells seeded at 20,000–60,0000 cells/well. Panel B: Basal RCR and Maximal RCR values were determined for the cells seeded at 40,000 cells/well. Data shown are the mean ± sem, n≥3 per group. *, $p<0.05$ vs. Basal RCR.

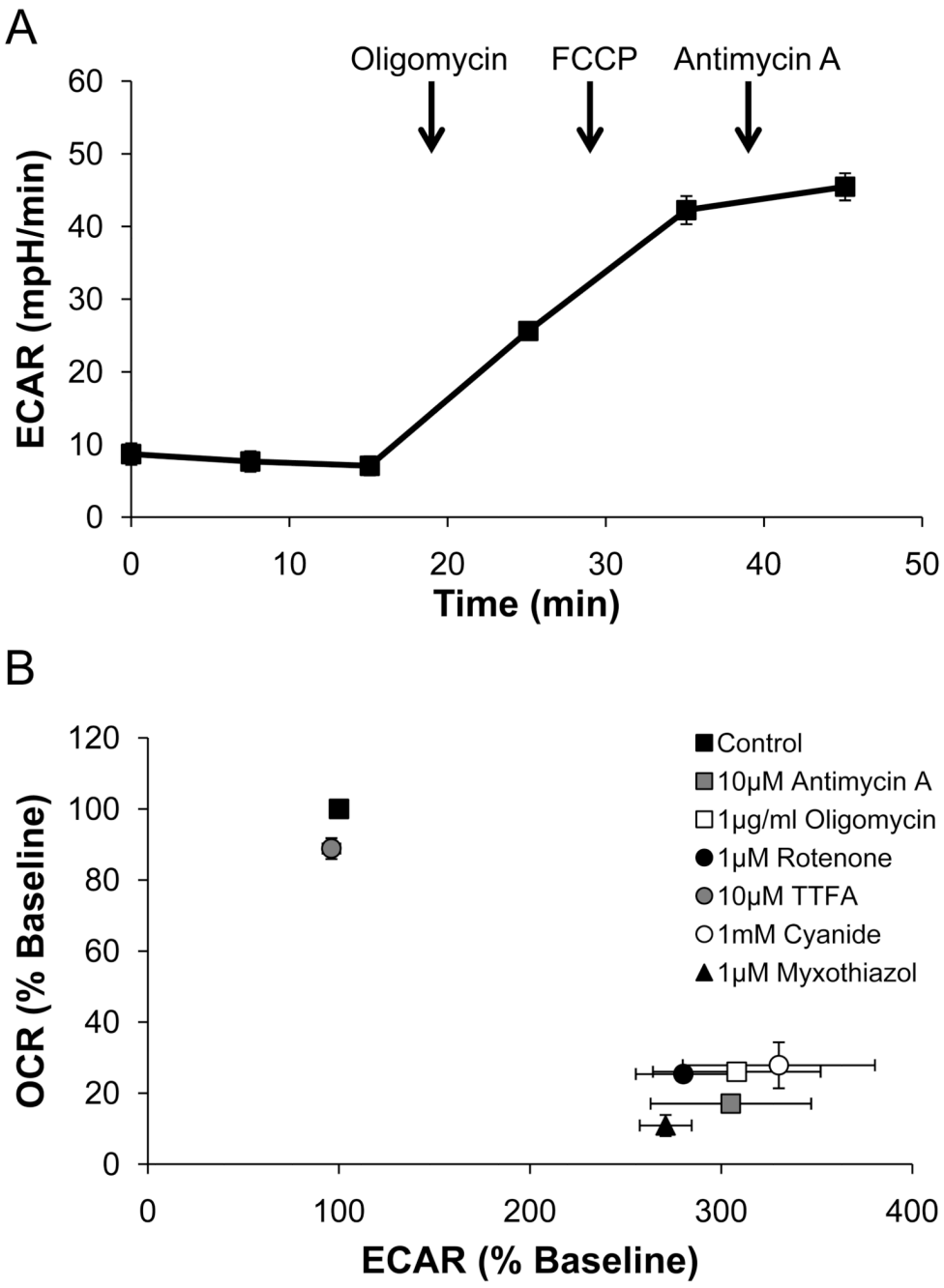

Figure 3. Bioenergetic profile of BAEC treated with inhibitors of mitochondrial oxygen consumption

BAEC were seeded at 40,000 cells/well and treated with 10 μM Antimycin A, 1 μg/ml oligomycin, 1 μM rotenone, 10 μM TTFA, 1 mM cyanide, or 10 μM myxothiazole and OCR and ECAR were measured. The resulting effects on OCR and ECAR are plotted as a percentage of the baseline measurement for each treatment. Data shown are the mean ± sem. n≥3 per treatment group.

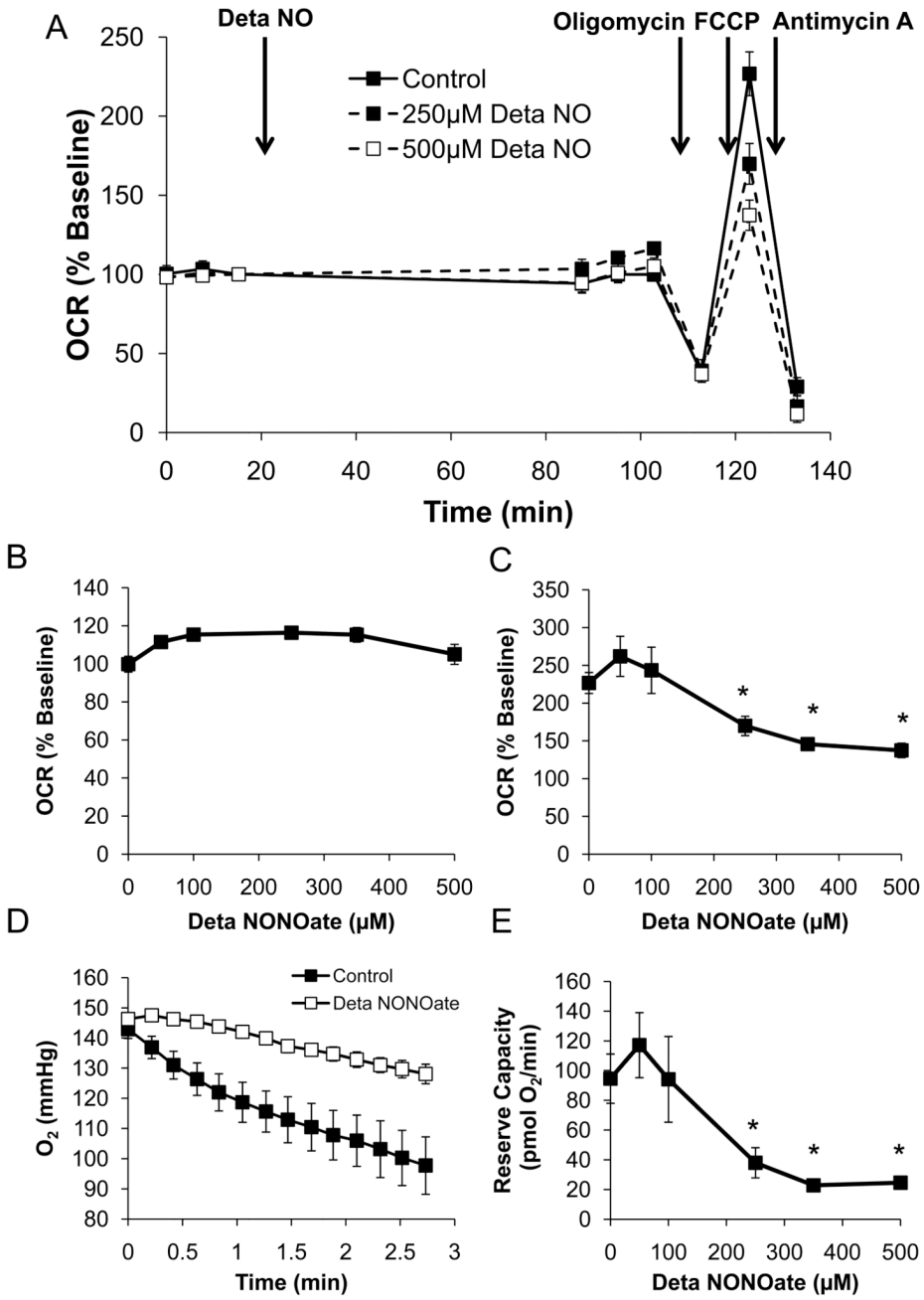

Figure 4. Acute nitric oxide treatment decreases reserve capacity, but has no effect on baseline oxygen consumption

BAEC were seeded at 40,000 cells/well and allowed to grow for 24 h. After a basal measurement of OCR, cells were treated without or with DetaNONOate (0–500 μM) for 1 h. Panel A: Representative traces for 0, 250, and 500 μM DetaNONOate. All cells were then treated sequentially with 1 μg/ml oligomycin, 1 μM FCCP and 10 μM antimycin A. Panel B: Effect of acute NO treatment on basal mitochondrial function. The third rate taken post-NO injection is plotted as a function of Deta NONOate concentration. Panel C: The change in FCCP-stimulated OCR is shown as a percentage increase from the original baseline and a function of Deta NONOate concentration. Panel D: Oxygen consumption as a result of

mitochondrial activity was plotted in the absence or presence of 500 μM Deta NONOate. Data shown are the measured oxygen concentrations during the OCR measurement taken immediately following FCCP injection. Panel E: Mitochondrial reserve capacity in cells treated with Deta NONOate. Data shown are the mean ± sem, n≥3 per group.

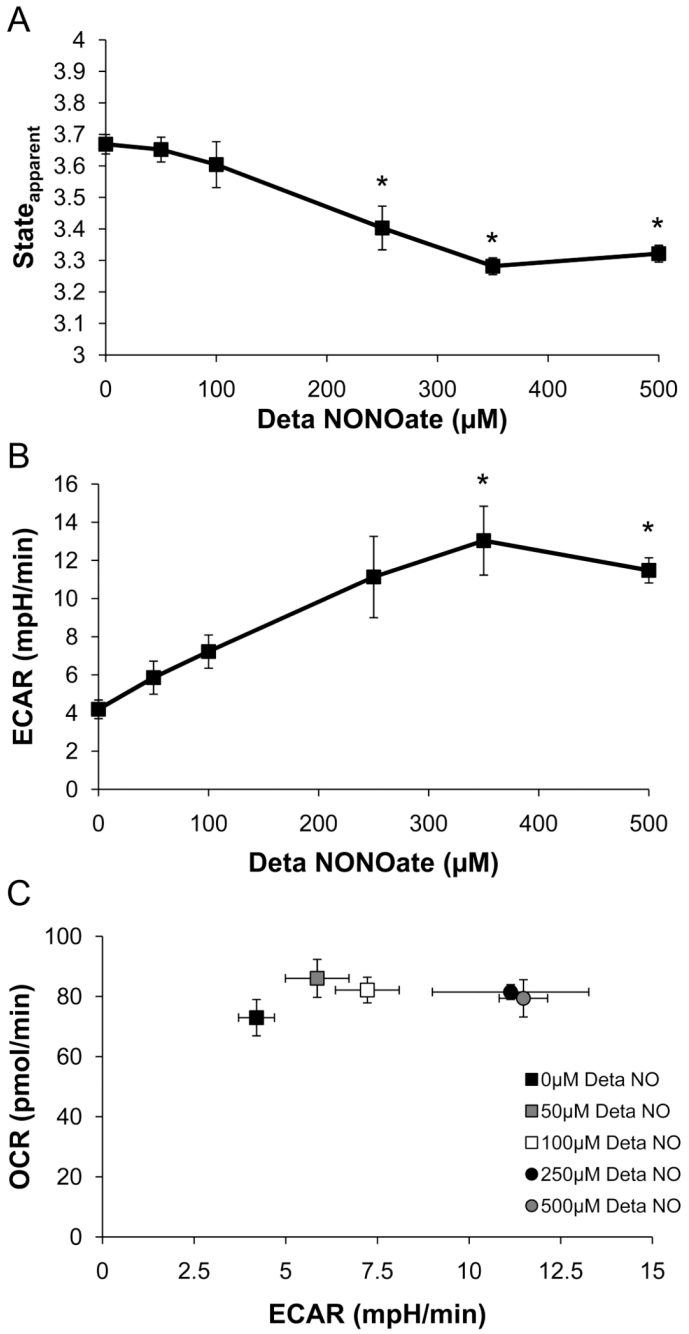

Figure 5. Acute nitric oxide decreases $State_{apparent}$ and increases the extracellular acidification rate

BAEC were seeded at 40,000 cells/well and allowed to grow for 24 h. Deta NONOate was injected at the indicated concentrations, and the cells were allowed to incubate for 1 h. The $State_{apparent}$ was calculated using the third post-NO injection rate as the basal rate. The data are plotted as a function of Deta NONOate concentration (Panel A). The basal ECAR was determined for each treatment group and is plotted as a function of Deta NONOate concentration (Panel B). The net effect on the metabolic profile was determined by plotting OCR vs. ECAR for each Deta NONOate concentration (Panel C). Data shown are the mean ± sem, n≥3 per group. *, $p<0.05$ vs. Control.

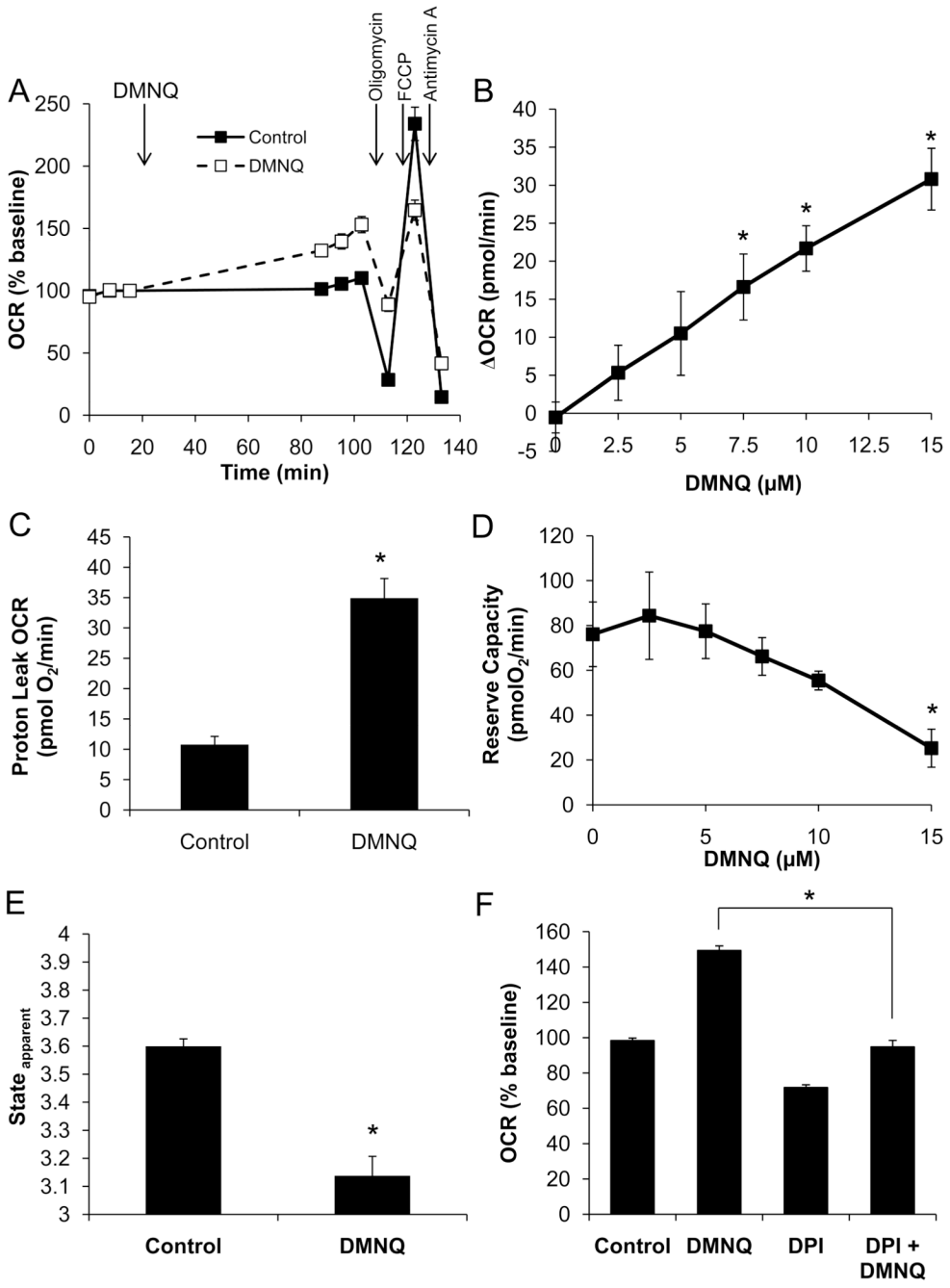

Figure 6. Acute DMNQ treatment decreases maximal OCR

BAEC were seeded at 40,000 cells/well and allowed to grow for 24 h. Three baseline measurements of OCR and ECAR were made, and then cells were treated with DMNQ (15 μM) for 1 h. Following this treatment, three further measurements were performed prior to sequential injection of oligomycin (1 μg/ml), FCCP (1 μM), and antimycin A (10 μM) to determine mitochondrial function (Panel A). Panel B: The increase in basal OCR due to DMNQ was determined and is plotted as a function of DMNQ concentration. Panel C: Proton leak was calculated and is shown for control and DMNQ (15 μM)-treated cells. Panel D: Reserve capacity following DMNQ treatment is also plotted as a function of DMNQ concentration. Panel E: Apparent respiratory state was calculated as described and is shown

for control and DMNQ (15 μM)-treated cells. Panel F: Diphenyleneiodonium (10 μM) was added with the DMNQ in some treatment groups. Inhibition of DMNQ-dependent OCR stimulation is shown. Data shown are the mean ± sem, n≥3 per group. *, $p<0.05$ vs. Control unless indicated otherwise.

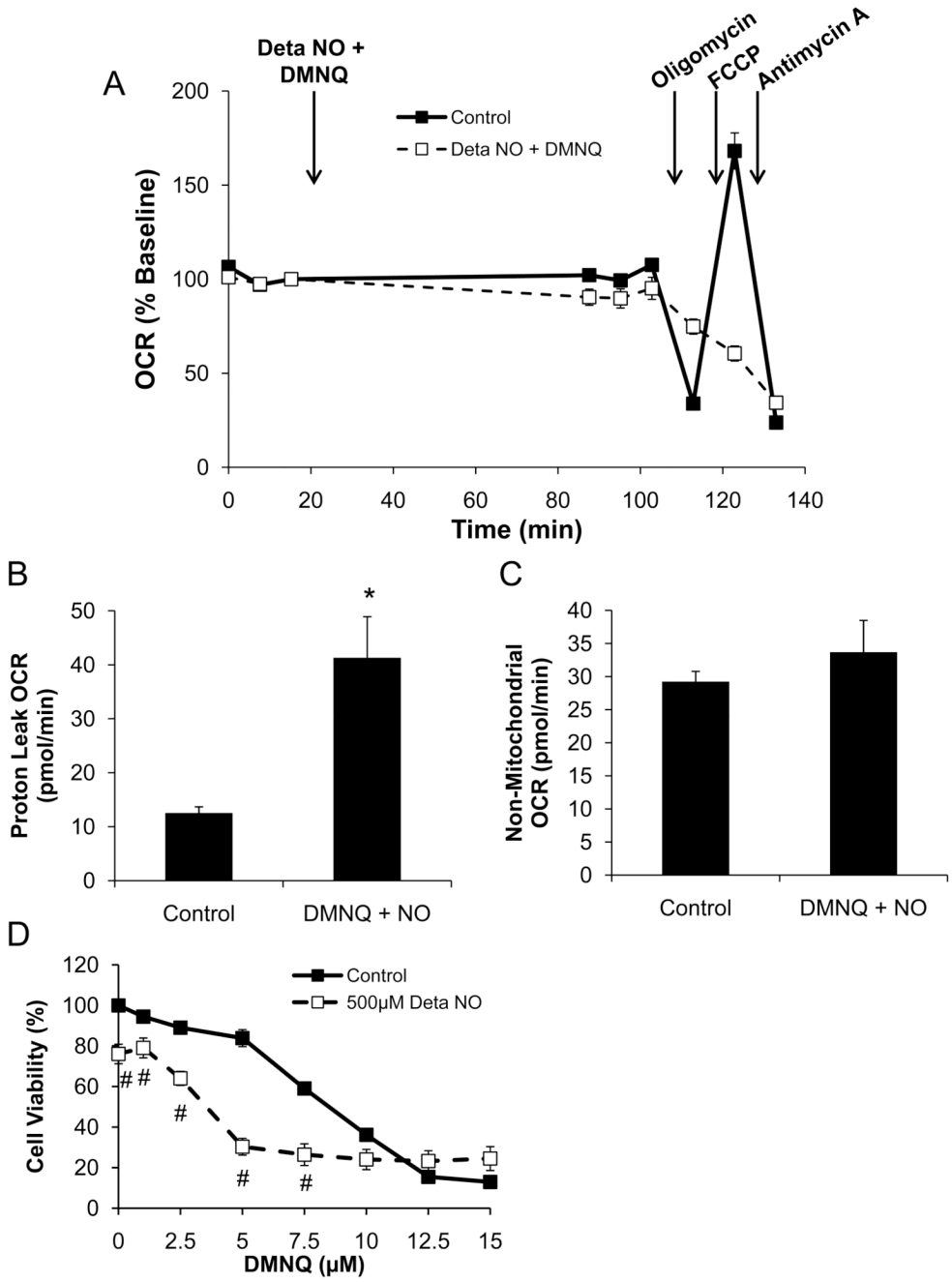

Figure 7. Proton leak is stimulated by combined Deta NONOate and DMNQ treatment

BAEC were seeded at 40,000 cells/well and allowed to grow for 24 h. Three baseline measurements of OCR and ECAR were made and then cells were treated with Deta NONOate (250 μM) and DMNQ (15 μM) combined for 1 h. Following this treatment, three further measurements were performed prior to sequential injection of oligomycin (1μg/ml), FCCP (1μM), and antimycin A (10 μM) to determine mitochondrial function. Panel B: Proton leak was calculated as the oligomycin-insensitive OCR minus the antimycin A-insensitive OCR. The non-mitochondrial, or antimycin A-insensitive OCR was also determined (Panel C). Panel D: Cell viability was determined using the MTT assay for cells treated with 500 μM Deta NONOate and the indicated concentration of DMNQ as a

cotreatment. Cell viability was calculated as a percentage of the control treated cells. Data shown are the mean ± sem, n≥3 per group. *, $p<0.05$ vs. Control. #, $p<0.05$ vs. matched concentration DMNQ-only control.

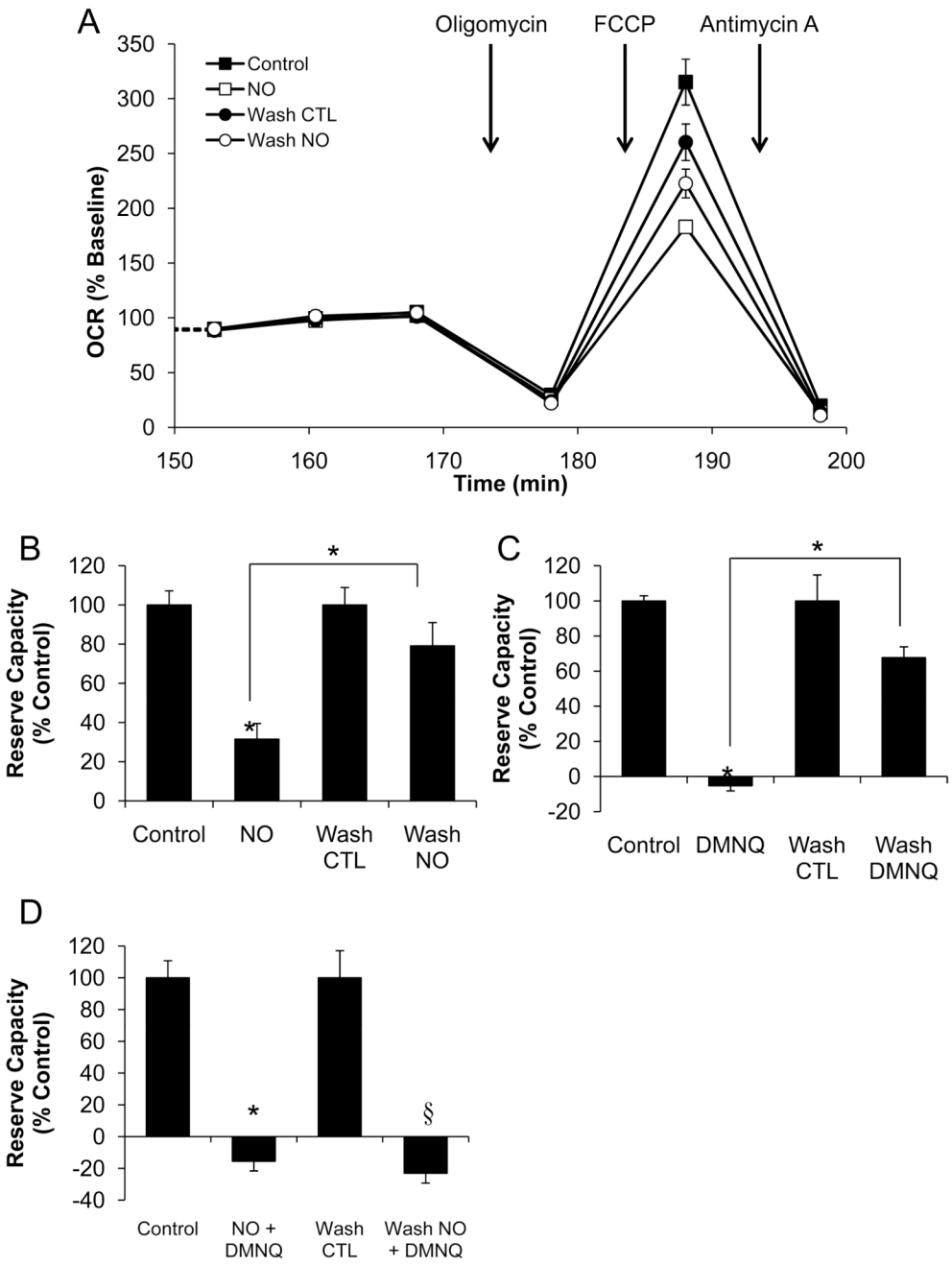

Figure 8. Reversal of OCR Inhibition is achieved following removal of Deta NONOate or DMNQ, but not these treatments combined

BAEC were seeded at 40,000 cells/well and allowed to grow for 24 h. Three baseline measurements of OCR were made, and then cells were treated with Deta NONOate (250 μM), DMNQ (15 μM), or both for 1 h. Following this treatment, three further measurements of OCR were performed. The plate was removed from the XF24, and the media changed to fresh assay media in the indicated groups. Three further measurements of basal OCR were then performed prior to sequential injection of oligomycin (1μg/ml), FCCP (1μM), and antimycin A (10 μM) to determine mitochondrial function. This portion of the experiment is shown in Panel A. Panel B: Reserve capacity was calculated for cells in the presence of Deta

NONOate, or with the NO donor removed. Panel C: Reserve capacity was calculated for cells in the presence of DMNQ, or with the DMNQ removed. Panel D: Reserve capacity was calculated for cells in the presence of Deta NONOate and DMNQ combined, or with these compounds removed. Data shown are the mean ± sem, n=5 per group. *, $p<0.05$ vs. Control. §, $p<0.05$ vs. Wash control.

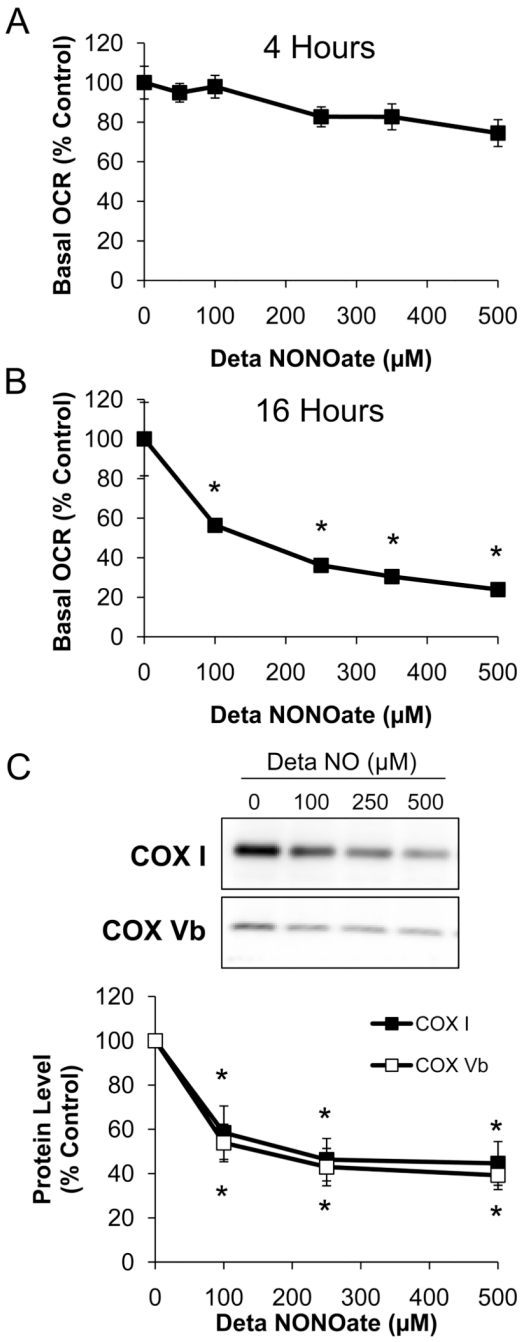

Figure 9. Chronic treatment with Deta NONOate decreases basal OCR

BAEC were seeded at 40,000 cells/well (Panel A), or 20,000 cells/well (Panel B) and allowed to grow for 24 hours. The cells were then treated with the indicated concentration of Deta NONOate for the indicated time. Basal OCR was then measured as described. Panel C: BAEC grown in 6-well plates were treated with the indicated concentration of Deta NONOate for 16 hours. Cells were lysed and harvested for protein analysis by SDS-PAGE and Western blotting. Representative blots for COX I and Vb are shown along with quantification of these proteins. Data shown are the mean ± sem. n≥3 per group. *, $p<0.05$ vs. Control.